Electronic Supplementary Material (ESI) for ChemComm.

Supporting Information

Aminotroponiminates as Tunable, Redox-Active Ligands: Reversible Single-Electron-Transfer and Reductive Dimerisation

C. Lichtenberg and I. Krummenacher*

Institut für Anorganische Chemie, Julius-Maximilians-Universität Würzburg, Am Hubland, 97074 Würzburg, Germany

Table of Contents

Experimental

General Considerations. All air- and moisture-sensitive manipulations were carried out using standard vacuum line Schlenk techniques or in an MBraun inert atmosphere dry-box containing an atmosphere of purified argon. Solvents were degassed and purified according to standard laboratory procedures. Starting materials were synthesised according to the literature.[1] NMR spectra were recorded on Bruker instruments operating at 400 or 500 MHz with respect to ^{1}H. ^{1}H and ^{13}C NMR chemical shifts are reported relative to $SiMe_4$ using the residual ^{1}H and ^{13}C chemical shifts of the solvent as a secondary standard. ^{23}Na NMR chemical shifts are reported relative to 1M NaCl in D_2O. In the NMR spectroscopic characterisation of ati and *di*-ati compounds, the CN$^{i\mathrm{Pr}}$ carbon atom is referred to as 1-C. Infrared spectra were collected on a Jasco FT/IR 6200 spectrometer. Elemental analyses were performed on a Leco or a Carlo Erba instrument. Cyclic voltammograms were recorded using a Gamry Instruments Reference 600 potentiostat. A standard three-electrode cell configuration was employed using a platinum disk working electrode, a platinum wire counter electrode, and a silver wire, separated by a *Vycor* tip, serving as the reference electrode. Formal redox potentials are referenced to the ferrocene/ferrocenium redox couple. UV-vis spectra were recorded with a Jasco V-660 UV-vis spectrometer. EPR measurements at X-band (9.37 GHz) were carried out at 298 K using a Bruker ELEXSYS E580 CW/FT EPR spectrometer. CW EPR spectra were measured using 1.6 mW microwave power and 0.1 G field modulation at 100 kHz, with a conversion time of 80 ms. The spectral simulations were performed using MATLAB 8.6 and the EasySpin 5.0.18 toolbox.[2] Single crystals suitable for X-ray diffraction were coated with polyisobutylene or perfluorinated polyether oil in a glove-box, transferred to a nylon loop and then transferred to the goniometer of a diffractometer equipped with a molybdenum X-ray tube (λ = 0.71073 Å). The structures were solved using direct methods (SHELXS) completed by Fourier synthesis and refined by full-matrix least-squares procedures. CCDC 1455872 contains the crystallographic information for this work.

Computational Details. DFT calculations were performed with the Gaussian program[3] using the 6-31G(d,p)[4] (H, C, N, O), the 6-311G(d,p)[5] (Na), or the LanL2DZ[6] (Rh) basis set and the B3LYP functional.[7] Frequency analyses of the reported structures showed no imaginary frequencies. Thermodynamic parameters were calculated at a temperature of 298.15 K and a pressure of 1.00 atm. Cartesian coordinates of optimised structures are provided as an xyz file.

Improved synthesis of 2. The yield of compound **2** could be increased to 88%, when the reaction was performed on larger scale (factor 2) and relative amounts of solvents used for washing and recrystallizing the product were reduced (factor 6). Analytical data were in full agreement with previously reported data.[1b]

In situ generation of [Na$_4$(*di*-ati$^{\mathrm{Ph}/i\mathrm{Pr}}$)(thf)$_n$] (4). Sodium sand (1.0 mg, 0.04 mmol) was added to a solution of **3** (13.0 mg, 0.04 mmol) in THF-d$_8$ (0.5 mL). The colour of the reaction mixture turned from yellow to deep red. The course of the reaction was monitored by ^{1}H NMR spectroscopy. Full conversion of **3** to give **4** was observed after 19 h with a selectivity of ≥95%. NMR data were in agreement with those of isolated **4** (*vide infra*).

Oxidation of in situ generated [Na$_4$(*di*-ati$^{\mathrm{Ph}/i\mathrm{Pr}}$)(thf)$_n$] (4) to give 3. [AgBF$_4$] (7.6 mg, 0.04 mmol) was added to a solution of in situ generated **4** in THF-*d*$_8$ (*vide supra*). The colour of the reaction mixture changed from deep red to yellow. ^{1}H NMR spectroscopic analysis of the reaction mixture indicated full conversion of **4** to give **3** with a selectivity of ≥95%.

^{1}H NMR data of **3** generated by oxidation of **4** were identical with those of isolated **3** prepared according to the literature[1b]: ^{1}H NMR (400 MHz, THF-*d*$_8$) δ = 1.16 (d, 6H, $^3J_{HH}$ = 6.2 Hz, Me), 1.76-1.79 (m, 4H, β-THF), 3.60-3.63 (m, 4H, α-THF), 3.79 (sept, 1H, $^3J_{HH}$ = 6.2 Hz, C*H*Me$_2$), 5.42 (br dd, 1H, $^3J_{HH}$ = 8.8 Hz, 5-H), 5.87 (d, 1H, $^3J_{HH}$ = 11.1 Hz, 7-H), 6.04 (d, 1H, $^3J_{HH}$ =

10.6 Hz, 3-H), 6.19 (br dd, 1H, $^3J_{HH}$ = 8.8 Hz, $^3J_{HH}$ = 11.1 Hz, 6-H), 6.41 (br dd, 1H, $^3J_{HH}$ = 8.8 Hz, $^3J_{HH}$ = 10.6 Hz, 4-H), 6.73, (m, 1H, $^3J_{HH}$ = 7.4 Hz, *p*-Ph, partially overlapping with *o*-Ph), 6.75 (m, 2H, $^3J_{HH}$ = 8.6 Hz, *o*-Ph, partially overlapping with *m*-Ph), 7.13 (br t, 2H, $^3J_{HH}$ = 7.7 Hz, *m*-Ph) ppm.

[Na_4(*di*-ati$^{Ph/iPr}$)(thf)$_n$] (4). Sodium sand (9 mg, 0.39 mmol) and hexanes (4 mL) were added to a solution of **3** (63 mg, 0.19 mmol) in THF (2 mL). The colour of the reaction mixture turned from yellow to deep red. After a few minutes a solid started to precipitate. After 2 d, the reaction mixture was filtered and the filtrate stored at –30 °C. A red crystalline solid precipitated from the filtrate after 2 d, which was isolated by filtration and dried in a stream of argon. Yield (determined for n = 2.33): 10 mg, 14 µmol, 15%.

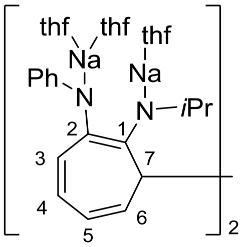

The amount of THF in the isolated compound has to be checked individually for every batch. Values ranging from n = 2 to n = 6 molecules of THF per formula unit have been observed.
^{1}H NMR (400 MHz, THF-d_8): δ = 0.56 (d, 6H, $^3J_{HH}$ = 6.0 Hz, Me^1), 0.78 (d, 6H, $^3J_{HH}$ = 6.0 Hz, Me^2), 1.76-1.79 (m, n×4H, β-THF), 3.60-3.62 (m, n×4H, α-THF), 3.70 (dd, 2H, $^3J_{HH}$ = 8.7 Hz, $^4J_{HH}$ = 4.2 Hz, 7-H), 4.25 (sept, 2H, $^3J_{HH}$ = 6.0 Hz, C*H*Me$_2$), 4.74 (dd, 2H, $^3J_{HH}$ = 8.5 Hz, $^3J_{HH}$ = 8.7 Hz, 6-H), 5.10 (dd, 2H, $^3J_{HH}$ = 6.6 Hz, $^3J_{HH}$ = 10.0 Hz, 4-H), 5.64 (t, 2H, $^3J_{HH}$ = 6.8 Hz, *p*-Ph), 6.01 (dd, 2H, $^3J_{HH}$ = 6.6 Hz, $^3J_{HH}$ = 8.5 Hz, 5-H), 6.22 (d, 2H, $^3J_{HH}$ = 10.0 Hz, 3-H), 6.34 (d, 2H, $^3J_{HH}$ = 8.3 Hz, *o*-Ph^1), 6.43 (d, 2H, $^3J_{HH}$ = 8.0 Hz, *o*-Ph^2), 6.59-6.62 (m, 2H, *m*-Ph^1), 6.61-6.64 (m, 2H, *m*-Ph^2) ppm. ^{13}C NMR (101 MHz, THF-d_8): δ = 20.72 (s, Me^1), 26.54 (s, β-THF), 28.28 (s, Me^2), 41.96 (s, 7-C), 45.43 (s, C*H*Me$_2$), 68.39 (s, α-THF), 99.98 (s, 4-C), 105.66 (s, *o*-Ph^2), 105.88 (s, *p*-Ph), 110.56 (s, 6-C), 119.40 (s, *o*-Ph^1), 123.55 (s, 2-C), 125.89 (s, 5-C), 129.10 (s, 3-C), 130.00 (s, *m*-Ph^2), 131.12 (s, *m*-Ph^1), 151.63 (s, 1-C), 163.06 (s, *ipso*-Ph) ppm. UV/VIS (THF): λ_{max} = 272, 355, 467 nm. Anal. calc. for $C_{32}H_{34}N_4Na_4\cdot(OC_4H_8)_{2.33}$ (734.86 g/mol): C, 67.56; H, 7.22; N, 7.62; found: C, 67.96; H, 7.41; N, 7.37.

C–C coupling of Grignard reagents with aryl bromides. In a representative protocol, the desired Grignard reagent was prepared by stirring a solution of the respective aryl bromide (0.223 mmol)[8] with an excess of Mg (1.2 mmol) in THF (1 mL) for 14 h. For the coupling reaction, the Grignard solution was separated from excess Mg by filtration, which was washed with THF (0.5 mL). A solution of the second aryl bromide (0.33 mmol) in THF (0.5 mL) was added to the combined liquid phases. A (pre-)catalyst (0.022 mmol) and further additives (as stated in the text) were added, if desired, and the reaction mixture was heated to 80°C in a closed vessel for 4 d. Subsequently, the reaction mixture was quenched with water, *n*-decane was added as an internal standard, and the mixture was analysed by GC/MS.

Attempted reaction of 2 with PhBr. A J. Young NMR tube was charged with **2** (9.0 mg, 20 µmol), PhBr (6.3 mg, 40 µmol), and THF-d_8 (0.5 mL). The reaction mixture was heated to 80°C for 5.5 d. No conversion of either compound could be detected by ^{1}H NMR spectroscopy.

NMR spectra

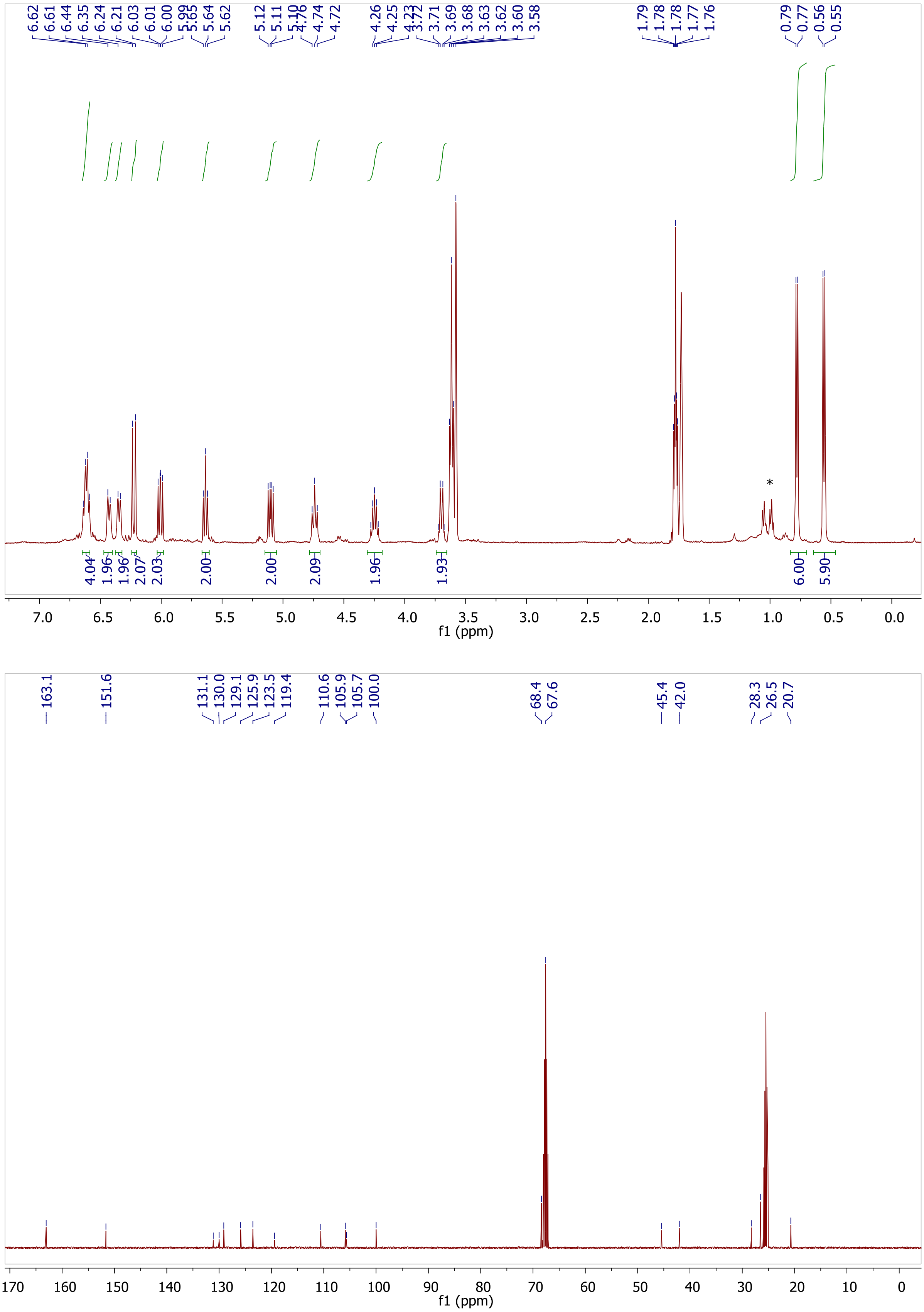

Figure S1. ^1H and ^{13}C NMR spectra of *in situ* generated **4** in THF-d_8. Resonances marked with an asterisk are due to small amounts of an isomer of **4**.

Reduction of compound 2

The reaction of **2** with a slight excess of elemental sodium at room temperature in dimethoxyethane was monitored by EPR spectroscopy. Under these conditions, a poorly resolved signal was detected, which is in contrast with the high resolution of hyperfine splittings that was observed for the reduction of **3** under identical conditions. When the reduction of **2** with Na was performed in THF as a solvent, a slightly broadened isotropic signal with g_{avg} = 2.003 could be observed (*vide infra*). The signal pattern was highly similar to the one that was detected in the reduction of compound **3** in THF. This is in agreement with the predominant localisation of spin density on the ligand backbone and the NPh group in the rhodium species ($[NaRh(ati^{Ph/iPr})(cod)(thf)_3]^{\bullet}$) as determined by DFT calculations (*vide infra* and main text).

In order to obtain further evidence for reversible electron transfer to a rhodium species under these conditions, the reduction of **2** with elemental sodium in THF was also monitored by cyclic voltammetry in THF/0.1 M $[(n\mathrm{Bu})_4N][PF_6]$ at room temperature in a separate experiment. In the potential window of – 3.0 to –0.5 V vs. Fc/Fc^+, only the reversible redox wave for the redox couple **2**/$[\mathbf{2}]^{\bullet -}$ at –2.69 V could be observed within reaction times ranging from 5 min to more than 4 h.

Attempts towards the isolation of a reduced species containing the radical anion $[\mathbf{2}]^{\bullet -}$ were so far unsuccessful. NMR spectroscopic investigation of a reaction mixture in which **2** had been exposed to a slight excess of Na for prolonged reactions times of ca. 19 h, revealed that the sodium compound **3** had formed in addition to other yet unidentified products.

Cyclic Voltammetry

Cyclic Voltammograms of 1. Cyclic voltammograms of [H-ati$^{Ph/iPr}$] (**1**) in THF/0.1 M $[N(nBu)_4][PF_6]$ at 23 °C show a partially reversible redox wave at –2.65 V vs. Fc/Fc$^+$ (*cf*, main text). This redox event becomes chemically reversible at high scan rates of ≥ 5 V·s^{-1} (Figure S2). In addition, an irreversible oxidation is observed at a potential of +0.39 V (Figure S3).

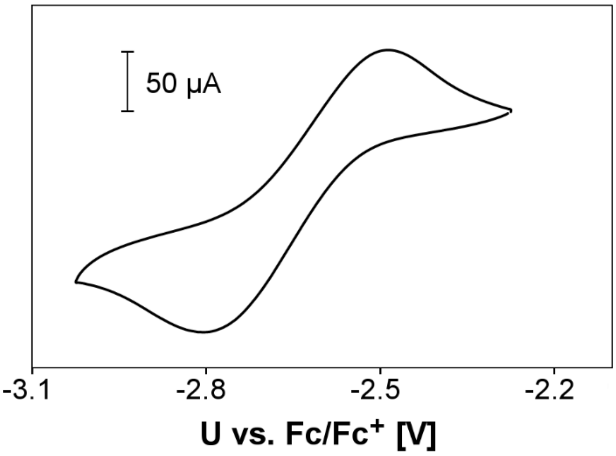

Figure S2. Cyclic voltammogram of [H-ati$^{Ph/iPr}$] (**1**) in THF/0.1 M $[N(nBu)_4][PF_6]$ at 23 °C and a scan rate of 5 V·s^{-1}.

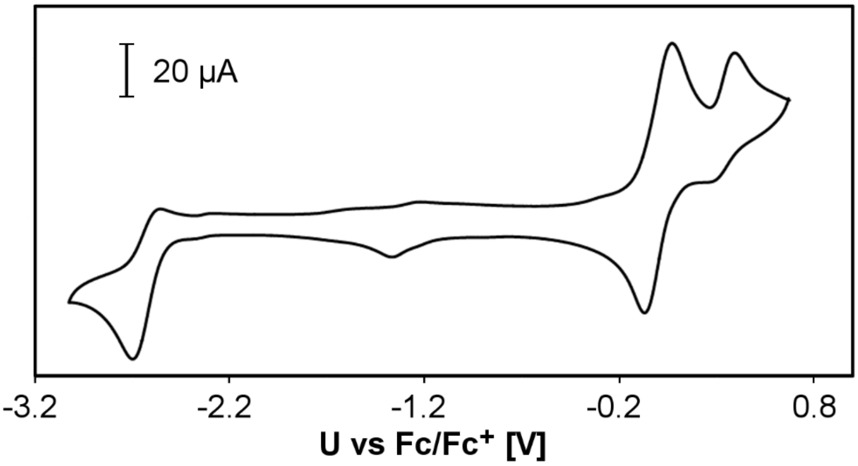

Figure S3. Cyclic voltammogram of [H-ati$^{Ph/iPr}$] (**1**) in THF/0.1 M $[N(nBu)_4][PF_6]$ at 23 °C and a scan rate of 250 mV·s^{-1} with ferrocene added as reference.

Cyclic Voltammograms of 2. Cyclic voltammograms of [Rh(ati$^{Ph/iPr}$)(cod)] (**2**) in THF/0.1 M [N(*n*Bu)$_4$][PF$_6$] at 23 °C show a reversible redox wave at –2.69 V vs. Fc/Fc$^+$ (*cf*, main text). The reversible character of the redox event is indicated by a linear correlation of the square root of the scan rate and the anodic and cathodic peak currents, respectively (Figure S4). Furthermore, compound **2** shows an irreversible oxidation at a potential of +0.18 V (Figure S5).

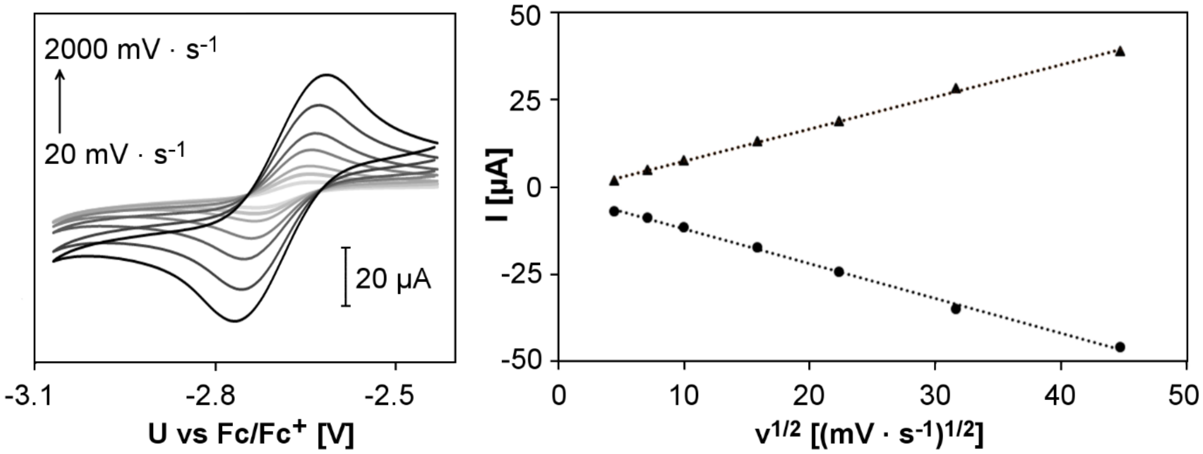

Figure S4. Left: Cyclic voltammogram of [Rh(ati$^{Ph/iPr}$)(cod)] (**2**) in THF/0.1 M [N(*n*Bu)$_4$][PF$_6$] at 23 °C and scan rates of 20-2000 mV·s^{-1}. Right: Plot of anodic (triangles) and cathodic (circles) peak current vs. square root of scan rate for cyclic voltammograms of **2**.

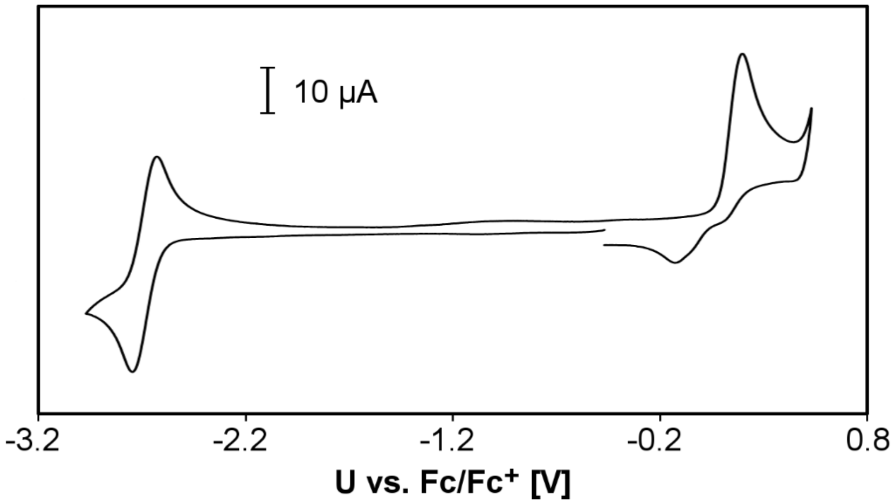

Figure S5. Cyclic voltammogram of [Rh(ati$^{Ph/iPr}$)(cod)] (**2**) in THF/0.1 M [N(*n*Bu)$_4$][PF$_6$] at 23 °C and a scan rate of 250 mV·s^{-1}.

Cyclic Voltammograms of 3. Cyclic voltammograms of [Na(ati$^{Ph/iPr}$)(thf)] (**3**) in THF/0.1 M [N(nBu)$_4$][PF$_6$] at 23 °C show a reversible reduction wave at –2.67 V vs. Fc/Fc$^+$ and a corresponding oxidation wave at –0.69 V vs. Fc/Fc$^+$ (*cf*, main text). Furthermore, compound **3** shows an irreversible oxidation at a potential of +0.42 V (Figure S6).

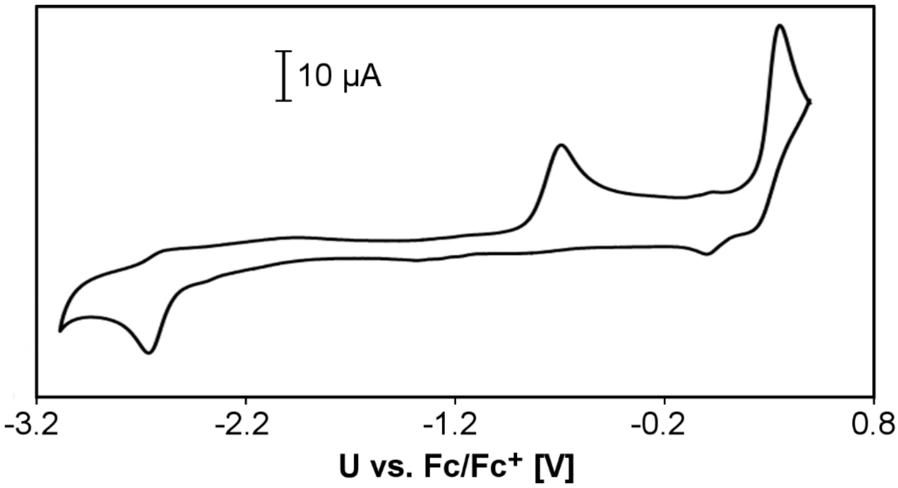

Figure S6. Cyclic voltammogram of [Na(ati$^{Ph/iPr}$)(thf)] (**3**) in THF/0.1 M [N(nBu)$_4$][PF$_6$] at 23 °C and a scan rate of 250 mV·s$^{–1}$.

Single Crystal X-ray Diffraction Analysis of 4

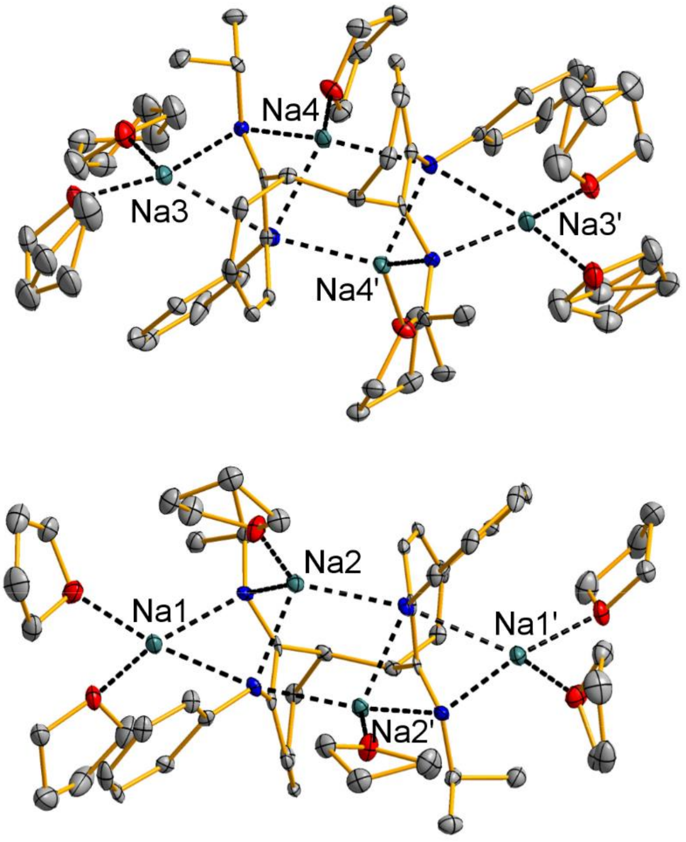

Figure S7. Molecular structure of **4** in the solid state. The asymmetric unit consists of two “half formula units”. The symmetry equivalent positions generating the other two “half formula units” are also shown. Displacement ellipsoids are shown at the 50% probability level. Hydrogen atoms are omitted for clarity.

EPR Spectroscopy

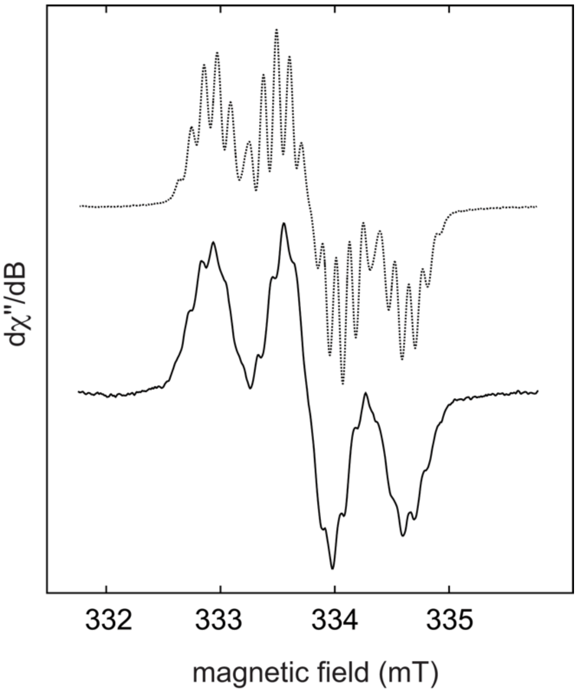

Figure S8. Continuous-wave X-band EPR spectra of the reduction of **3** with sodium metal, recorded in DME (*top*) and THF (*bottom*) solution.

DFT Calculations

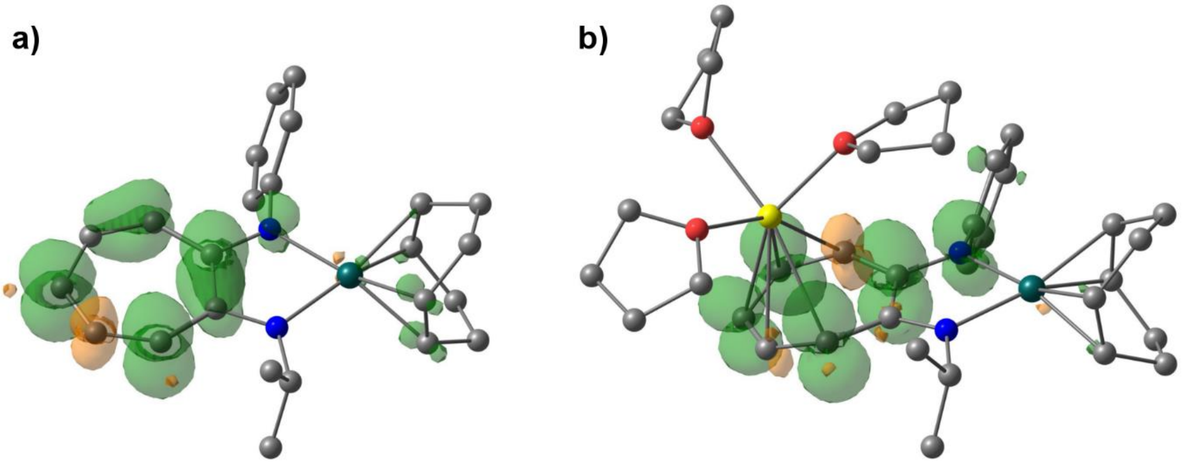

Figure S9. Calculated structures of a) [Rh(ati$^{Ph/iPr}$)(cod)]$^{\bullet -}$ and b) [NaRh(ati$^{Ph/iPr}$)(cod)(thf)$_3$]$^{\bullet}$ with spin density at isovalues of 0.0025 (α-spin: green, β-spin: orange). Hydrogen atoms are omitted for clarity. Colour code for atoms: grey = C; blue = N; red = O; yellow = Na; teal = Rh.

Table S1. Calculated free energies (G°, hartree) and enthalpies (H°, hartree) of Na and optimised structures.

Compound	H° [hartree]	G° [hartree]
$[\mathrm{Rh}(\mathrm{ATI}^{\mathrm{Ph}/i\mathrm{Pr}})(\mathrm{cod})]^{\bullet -}$	–1150.559339	–1150.641419
$[\mathrm{NaRh}(\mathrm{ATI}^{\mathrm{Ph}/i\mathrm{Pr}})(\mathrm{thf})_3]$	–2009.904572	–2010.043370
Na	–162.284269	–162.301713
$[\mathrm{Na}(\mathrm{ATI}^{\mathrm{Ph}/i\mathrm{Pr}})(\mathrm{thf})_3]$	–1588.508018	–1588.625600
$[\mathrm{Na}_2(\mathrm{ATI}^{\mathrm{Ph}/i\mathrm{Pr}})(\mathrm{thf})_3]$	–1750.819345	–1750.944433
$[\mathrm{Na}_2(\mathrm{ATI}^{\mathrm{Ph}/i\mathrm{Pr}})(\mathrm{thf})_4]$	–1983.172409	–1983.312832
$[\mathrm{Na}_4(di\text{-}\mathrm{ATI}^{\mathrm{Ph}/i\mathrm{Pr}})(\mathrm{thf})_6]$	–3501.684444	–3501.902456

Catalysed C–C coupling of Grignard reagents with aryl bromides

Recently, Shirakawa, Hayashi, *et al.* reported on the catalyst-free C–C coupling of aryl Grignard reagents with aryl halides.[9] Three different single electron transfer steps are suggested to be involved in this reaction.[9b] Importantly, it was also shown that in accordance with the proposed mechanism, the presence of a single electron transfer catalyst can enhance the rate of reaction.[9a] For instance, the reaction between a phenyl Grignard reagent, PhMgBr, and 2-bromonaphthalene gave only traces of the C–C coupling product at reaction temperatures of 80°C, whereas 80% of the coupling product could be detected when the reaction was performed in the presence of 20 mol% of the radical lithium 4,4’-di-tert-butylbiphenylide.

The cyclic voltammograms of the H-ati$^{\mathrm{Ph}/i\mathrm{Pr}}$ ligand and its derivatives show that these compounds can undergo well-defined single electron transfer events. The above-mentioned transformation (C–C coupling of a phenyl Grignard reagent with 2-bromonaphthalene) was chosen as a model reaction to investigate if compounds based on the ati$^{\mathrm{Ph}/i\mathrm{Pr}}$ ligand can act as single electron transfer catalysts (see reaction scheme in Table S2).

Whereas a mixture of toluene and THF had been determined as the optimised solvent for the catalyst-free coupling reaction in the literature,[9a] we chose THF as a solvent in order to ensure solvation of all potential catalyst species. Under these slightly modified reaction conditions, only traces of the C–C coupling product **6** could be detected without the addition of a catalyst after reaction times of 4 d (Table S2, entry 1). When 10 mol% of compound **1** were added to the reaction mixture, significant amounts of the coupling product **6** were formed (0.025 mmol, 11% with respect to PhMgBr, entry 2). In addition, the homo-coupling product **7** was also detected (0.013 mmol, 12% with respect to PhMgBr). The formation of homo-coupling side products is commonly observed in (intended) cross coupling reactions between Grignard reagents and aryl/allyl halides that proceed via a single electron transfer mechanism.[9,10] These results provide a proof of concept concerning the utilisation of ati-species as single electron transfer catalysts.

Compound **3** or a stoichiometric mixture of **3** and $[(n\mathrm{Bu})_4\mathrm{N}]\mathrm{Cl}$ showed a lower catalytic activity under identical conditions (not included in Table S2).

The rhodium species **2** undergoes reversible electron transfer under cyclic voltammetry conditions. Accordingly, **2** was also tested as a catalyst in the reaction of PhMgBr with 2-bromonaphthalene. Under identical conditions, virtually quantitative conversion of the Grignard reagent was observed (entry 3), with formation of the cross-coupling product **6** (0.10 mmol) and the homo-coupling product **7** (0.061 mmol). However, it has to be pointed out that a mechanism operating via oxidative addition / transmetalation / reductive elimination cannot be ruled out, although it is considered rather unlikely for a robust Rh species with two strongly bound chelating ligands (*vide infra*).

Table S2. Reaction of PhMgBr with 2-bromonaphthalene.

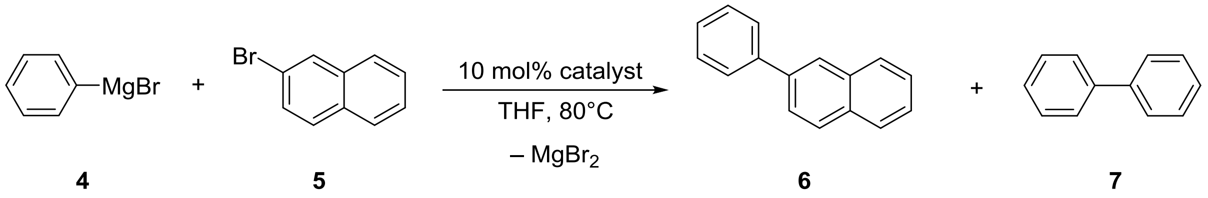

Entry	Cat.	PhMgBr [mmol]	Conversion of PhMgBr [mmol]	Yield of Products[a] [mmol]	
				6	**7**
1	none	0.223	traces	traces	not detected
2[11]	**1**	0.223	0.051	0.025	0.013
3	**2**	0.223	0.22	0.10	0.061

Conditions: i) PhBr (entries 1, 3: 0.223 mmol; entry 2: 0.245 mmol),[11] Mg (1.2 mmol), 14 h; ii) 2-bromonaphthalene (0.332 mmol), catalyst if present (0.022 mmol), THF (2 mL), 80°C, 4 d. a: determined by GC/MS using *n*-decane as an internal standard.

C–C couplings between aryl Grignard reagents and aryl bromides catalysed by ati$^{Ph/iPr}$ species were further investigated using the more efficient catalyst **2**. Reaction of PhMgBr with PhBr catalysed by 10 mol% **2** gave the coupling product biphenyl (**9**) in 72% yield (Table S3, entry 1), whereas only 4% **9** were detected in the absence of a catalyst (entry 2). The catalysed reaction still gave significant yields, when performed in the presence of excess mercury (40 equiv. with respect to catalyst), indicating that small Rh particles are unlikely to be the catalytically active species.[12] In order to obtain indications whether the catalysed reaction might proceed via a mechanism involving oxidative addition of PhBr to the Rh centre in **2**, the aryl bromide and compound **2** were heated to 80°C in a 2:1 molar ratio using THF-d_8 as a solvent. After reaction times of >5 d, no indications for a reaction between PhBr and **2** could be obtained by ^{1}H NMR spectroscopy.

Table S3. Catalysed reactions of aryl Grignard reagents with aryl bromides.

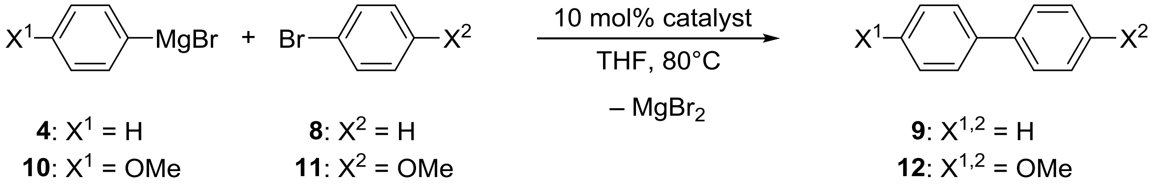

Entry	Cat.	Substrates		Product	Yield[a] [%]
		X^1	X^2		
1	**2**	H	H	**9**	72
2	none	H	H	**9**	4
3	**2**	OMe	OMe	**12**	41
4	none	OMe	OMe	**12**	2

Conditions: i) ($X^1C_6H_4Br$) (0.22 mmol), Mg (1.2 mmol), 14 h; ii) ($X^2C_6H_4Br$) (0.332 mmol) catalyst if present (0.022 mmol), THF (2 mL), 80°C. a: determined by GC/MS using *n*-decane as an internal standard.

Using a Grignard reagent and an aryl bromide with OMe substituents in *para*-positions as electron rich substrates gave the coupling product **12** in lower yields of 41% for the catalysed reaction (entry3). In the non-catalysed control reaction, **12** was detected in only 2% yield (entry 4).

In order to investigate the electronic demand of the coupling reaction with respect to the aryl bromide component alone, PhMgBr was reacted with an electron rich arene (*p*-OMe-C_6H_4Br) and with an electron poor arene (*p*-CF_3-C_6H_4Br) (Table S4). For comparison, the results that were obtained with PhBr as the arene component are also listed in Table S4. Overall, the highest yields (72%) were obtained using PhBr as the arene component (entry 1). The conversions of the Grignard reagent were 40% and 45%, when using an electron rich or electron poor arene component, respectively (entries 2,3). However, the product distribution between the cross-coupling and the homo-coupling product in these reactions is distinct. Whereas the formation of the homo-coupling product was favoured in the first case by a factor of 1.9 (entry 2), this ratio is reversed in the second case (entry 3). These results are in line with a putative single electron transfer from a Grignard reagent or a reduced catalyst species to *p*-CF_3-C_6H_4Br being more facile than to *p*-OMe-C_6H_4Br.[9b]

Table S4. Catalysed reactions of aryl Grignard reagents with aryl bromides.

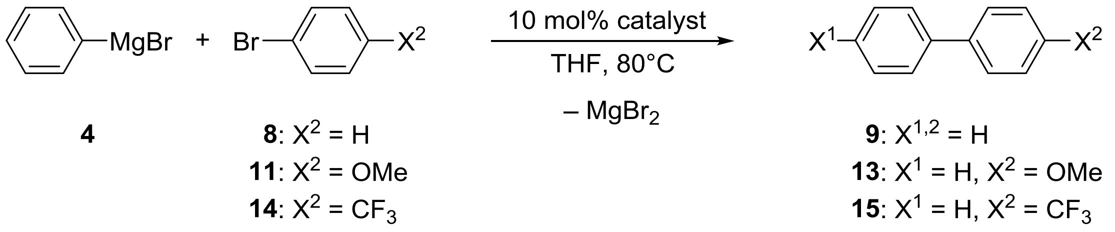

Entry	Cat.	ArylMgBr [mmol]	Conv. ArylMgBr [mmol]	Substrates		Yield[a] [mmol]	
				X^1	X^2	X^1/X^2	X^1/X^1
1	**2**	0.223	0.16	H	H	0.16	= X^1/X^2
2	**2**	0.223	0.090	H	OMe	0.031	0.059
3	**2**	0.223	0.10	H	CF_3	0.067	0.036

Conditions: i) ($X^1C_6H_4Br$) (0.223 mmol), Mg (1.2 mmol), 14 h; ii) ($X^2C_6H_4Br$) (0.332 mmol) catalyst if present (0.022 mmol), THF (2 mL), 80°C. a: determined by GC/MS using *n*-decane as an internal standard.

In summary, the results of this preliminary catalytic study show that ati-species can be utilised as single electron transfer catalysts, as indicated by the use of H-ati$^{Ph/iPr}$ as a pre-catalyst. Better results were obtained with the electrochemically more robust Rh species **2**. However, a mechanism operating via oxidative addition / transmetalation / reductive elimination has to be considered in this case. Although no indications for the feasibility of an oxidative addition could be obtained, this scenario could not strictly be ruled out.

References

1 (*a*) M. Dochnahl, K. Löhnwitz, J.-W. Pissarek, M. Biyikal, S. R. Schulz, S. Schön, N. Meyer, P. W. Roesky and S. Blechert, *Chem. Eur. J.*, 2007, **13**, 6654; (*b*) C. Lichtenberg, *Organometallics*, 2016, **35**, 894.

2 S. Stoll and A. Schweiger, *J. Magn. Reson.,* 2006, **178**, 42.

3 Gaussian 09, Revision or B.01 or D.01, M. J. Frisch, G. W. Trucks, H. B. Schlegel, G. E. Scuseria, M. A. Robb, J. R. Cheeseman, G. Scalmani, V. Barone, B. Mennucci, G. A. Petersson, H. Nakatsuji, M. Caricato, X. Li, H. P. Hratchian, A. F. Izmaylov, J. Bloino, G. Zheng, J. L. Sonnenberg, M. Hada, M. Ehara, K. Toyota, R. Fukuda, J. Hasegawa, M. Ishida, T. Nakajima, Y. Honda, O. Kitao, H. Nakai, T. Vreven, J. A. Montgomery, Jr., J. E. Peralta, F. Ogliaro, M. Bearpark, J. J. Heyd, E. Brothers, K. N. Kudin, V. N. Staroverov, R. Kobayashi, J. Normand, K. Raghavachari, A. Rendell, J. C. Burant, S. S. Iyengar, J. Tomasi, M. Cossi, N. Rega, J. M. Millam, M. Klene, J. E. Knox, J. B. Cross, V. Bakken, C. Adamo, J. Jaramillo, R. Gomperts, R. E. Stratmann, O. Yazyev, A. J. Austin, R. Cammi, C. Pomelli, J. W. Ochterski, R. L. Martin, K. Morokuma, V. G. Zakrzewski, G. A. Voth, P. Salvador, J. J. Dannenberg, S. Dapprich, A. D. Daniels, Ö. Farkas, J. B. Foresman, J. V. Ortiz, J. Cioslowski and D. J. Fox, Gaussian, Inc., Wallingford CT, 2009.

4 Hariharan, P. C.; Pople, J. A. *Theor. Chim. Acta*, 1973, **28**, 213.

5 (*a*) A. D. McLean and G. S. Chandler, *J. Chem. Phys.*, 1980, **72**, 5639; (*b*) K. Raghavachari, J. S. Binkley, R. Seeger and J. A. Pople, *J. Chem. Phys.*, 1980, **72**, 650.

6 (*a*) T. H. Dunning Jr., and P. J. Hay, in *Modern Theoretical Chemistry,* Ed. H. F. Schaefer III,; Vol. 3 (Plenum, New York, **1977**) 1-28; (*b*) P. J. Hay and W. R. Wadt, *J. Chem. Phys.*, 1985, **82**, 270; (*c*) P. J. Hay and W. R. Wadt, *J. Chem. Phys.*, 1985, **82**, 299.

7 A. D. Becke, *J. Chem. Phys.,* 1993, **98**, 5648.

8 The only exception was for entry 2 in Table S2, where 0.245 mmol of PhBr were used for the preparation of the Grignard reagent (see footnote 11).

9 (*a*) E. Shirakawa, Y. Hayashi, K. Itoh, R. Watabe, N. Uchiyama, W. Konagaya, S. Masui, T. Hayashi, *Angew. Chem. Int. Ed.,* 2012, **51**, 218; (*b*) N. Uchiyama, E. Shirakawa, T. Hayashi, *Chem. Commun.*, 2013, **48**, 364.

10 The formation of the homo-coupling product could be due to reaction of $[\mathrm{PhMgBr}]^{\bullet +}$ with PhMgBr or to Mg/Br exchange on 2-bromonaphthalene (see ref. 9)

11 The Grignard reagent (in this case: 0.245 mmol) is expected to rapidly react with **1** (0.022 mmol) under arene elimination. The remaining Grignard reagent (0.223 mmol) can act as a substrate in the C-C coupling reaction.

12 For literature on selective catalyst poisoning aiming at the distinction between homogeneously and heterogeneously operating catalysts see for instance: R. H. Crabtree, *Chem. Rev.*, 2012, **112**, 1536.